Status of the HOLMES Experiment

M. Faverzani[1,2] · B. Alpert[3] · M. Balata[4] · D. Backer[3] · D. Bennet[3] ·
A. Bevilaqua[6] · M. Biasotti[5,6] · M. Borghesi[1,2] · G. Ceruti[2] · M. De Gerone[6] ·
R. Dressler[7] · E. Ferri[1,2] · J. Fowler[3] · G. Gallucci[6] · J. Gard[3] · F. Gatti[5,6] ·
A. Giachero[1,2] · S. Heinitz[7,11] · G. Hilton[3] · U. Köster[8] · M. Lusignoli[9] ·
J. Mates[3] · E. Maugeri[7] · S. Nisi[4] · A. Nucciotti[1,2] · L. Parodi[6] · G. Pessina[2] ·
A. Puiu[1,2] · S. Ragazzi[1,2] · C. Reintsema[3] · M. Ribeiro-Gomez[10] · D. Schmidt[3] ·
D. Schumann[7] · F. Siccardi[5,6] · D. Swetz[3] · J. Ullom[3] · L. Vale[3]

Abstract

The absolute neutrino mass is still an unknown parameter in the modern landscape
of particle physics. The HOLMES experiment aims at exploiting the calorimetric
approach to directly measure the neutrino mass through the kinematic measurement
of the decay products of the weak process decay of ^{163}Ho. This low energy decay-
ing isotope, in fact, undergoes electron capture emitting a neutrino and leaving the
daughter atom, ^{163}Dy*, in an atomic excited state. This, in turn, relaxes by emitting
electrons and, to a considerably lesser extent, photons. The high-energy portion of
the calorimetric spectrum of this decay is affected by the non-vanishing neutrino
mass value. Given the small fraction of events falling within the region of interest,
to achieve a high experimental sensitivity on the neutrino mass, it is important to
have a high activity combined with a very small undetected pileup contribution. To
achieve these targets, the final configuration of HOLMES foresees the deployment
of a large number of ^{163}Ho ion-implanted TESs characterized by an ambitiously high
activity of 300 Hz each. In this paper, we outline the status of the major tasks that
will bring HOLMES to achieve a statistical sensitivity on the neutrino mass as low
as 2 eV/c^2.

Keywords Neutrino mass · Transition edge sensors · Electron capture

---

✉ M. Faverzani
   marco.faverzani@mib.infn.it

Extended author information available on the last page of the article

1 Introduction

The non-vanishing value of the neutrino mass has been indisputably demonstrated through the observation of the neutrino flavor oscillation phenomenon. The absolute value of the mass of this elusive particle, though, is still subject of several research activities. The study of the end point of a beta or electron capture decaying nucleus is the only model-independent experimental tool for accessing this quantity.

To date, the most sensitive approach to investigate the neutrino mass (m_ν) is through electromagnetic spectrometers. Belonging to this class of experiments, KATRIN (Karlsruhe Tritium Neutrino Experiment) will provide a sensitivity on the neutrino mass of 0.2 [1] eV/c^2, improving the current sensitivity by one order of magnitude, and reaching the ultimate technological limit for what concerns spectrometers. This experiment investigates the beta decay of a gaseous molecular tritium source by selecting the electrons close in energy to the end point through a MAC-E filter (Magnetic Adiabatic Collimation combined with an Electrostatic Filter): This technique allows the achievement of a large statistics in the region of interest (ROI). Nevertheless, the fact that the source is not enclosed inside the detector potentially introduces systematics, mostly related to the missing energy of decays on excited states and to the transport of the electrons from the source to the detector.

The calorimetric approach, despite the lower sensitivity achieved so far [2], has the potentiality to work around the issues caused by a beta emitter external to the detector: The idea consists in embedding the source in the active volume of a low temperature detector, such that the energy of the decay products is converted into heat and measured by a sensitive thermometer. On the one hand, this configuration allows the detection of the entire energy of the decay, except for the fraction carried away by the neutrino. On the other hand, calorimetry requires the acquisition of the entire spectrum, creating a non-negligible contribution due to pileups. Given that the fraction of events affected by pileup is $f_{pp} \approx A\tau_R$, where A is the activity of the decaying isotope per detector and τ_R is the time resolution of the detector, in order to keep the artifact due to these events as small as possible, the ideal experimental setup foresees a large isotope activity spread over a large number of fast detectors working in parallel [3].

In order to maximize the statistics in the region of interest, decays characterized by low transition energies Q are preferable. Among weak decay processes, ^{187}Re and ^{163}Ho display two of the lowest Q in nature. Despite past investigation of ^{187}Re [4], this isotope proved not to be fully compatible with the technical requirements of a high sensitivity neutrino mass measurement experiment, mostly due to the low specific activity and the relative slowness of the thermalization process of materials containing this isotope. For these reasons, the focus of the community has shifted to ^{163}Ho [5]. This latter isotope decays via electron capture on ^{163}Dy with a conveniently low Q of 2.8 keV [6]. The proximity of the M1 resonance to the end point enhances the statistics in the ROI.

HOLMES [7] will exploit the calorimetric approach to investigate the electron capture decay of ^{163}Ho through the deployment of 1000 transition edge sensors

capable of an energy and time resolutions of the order of the eV and of the μs, respectively. The activity of ^{163}Ho per detector will be of 300 Hz, so that a total statistics of 3×10^{13} events will be accumulated within 3 years of data taking. This statistics will allow HOLMES to achieve a statistical sensitivity on m_ν of ~ 2 eV/c^2 and establish the scalability of this approach to eventually achieve sub-eV sensitivities. A preliminary measurement of an array of 16 detectors is planned to start during the year 2020.

2 Transition Edge Sensors for HOLMES

The detectors' performance is a crucial factor in achieving the best obtainable sensitivity in HOLMES. The ideal detecting technology must provide four main features: high energy and time resolution, high multiplex ability and the ability to embed the ^{163}Ho source with a good efficiency. Transition edge sensors (TES) in combination with microwave multiplexing readout comply with all the aforementioned requirements. While the high energy resolution capability of TESs is well established, the requirement of a fast timing profile sets strict constraints on the readout bandwidth and on the design of the detectors. The rise time, which affects the effective time resolution achievable and ultimately the sensitivity of the experiment, is set by the available electrical bandwidth, depending upon the L/R ratio, where L is the inductance in the biasing circuit and R is the resistance of the TES at the working point. This bandwidth, however, has to match the bandwidth of the readout chain, in order to not run into slew rate issues. This condition effectively sets a minimum value for the rise time. On the other hand, the decay time of the pulses affects the *dead time*; [1] this quantity is determined, to first order, by the ratio C/G, where C and G are the heat capacity of the TES and its thermal conductance toward the bath, respectively. While C is set by requiring the full containment of the decay energy inside the absorber, G is the only tunable parameter for shortening the decay time. In HOLMES detectors, this is accomplished by increasing the thermal radiation through a copper structure which surrounds the whole detector [8].

After an extensive testing phase, the final detector geometry has been identified, showing a full width at half maximum (FWHM) energy resolution of (4.5 ± 0.3) eV at 2.6 keV [9] obtained with an exponential rise time of 14 μs.

---

[1] Two events happening in a time interval greater than the time resolution are recognized as pileups if the second pulse occurs on the decay of the first. In these cases, the safest analysis approach is to discard both events, causing a dead time due to the loss of a fraction of events which is equal to few times the product between the activity and the decay time.

3 Readout

The readout of the detectors for HOLMES is made with the microwave multiplexing scheme [11–13]. Each detector is coupled to a rf-SQUID (Superconducting Quantum Interference Device), which in turn is inductively coupled to a $\lambda/4$ resonator, such that variation in the temperature of the TES is translated into variation in flux in the SQUID, which ultimately varies the mutual inductance with the resonator, modifying its resonant frequency.

Each detector is coupled to a resonator designed to oscillate at a unique frequency, in the GHz range. Several resonators are capacitively coupled to a common feedline, so a single line enables the readout of several detectors. A comb of signals with frequencies tuned to the resonant frequencies of the resonators is generated by a digital-to-analog converter (DAC) at frequencies of the order of few MHz (baseband) and up-converted by mixing them with a GHz signal (local oscillator—LO). At the output from the resonator chip, these signals are down-converted by mixing them with the LO, channelized, acquired by an analog-to-digital converter and processed for real-time reconstruction of the TES signals. The generation of the baseband signal, the channelization, and the processing for the real-time demodulation is done by a ROACH2 (Reconfigurable Open Architecture Computing Hardware) board [14], while the up- and down-conversion is performed by a semi-custom commercial board produced to meet HOLMES readout requirements: In particular, it shows a conversion loss of − 7 dB, a value compatible for reading out 32 resonators.

The ADC/DAC boards which equip the ROACH2 provide a bandwidth of 500 MHz: Requiring a rise time for each detector of ∼ 10 µs up to 36 TESs can be read simultaneously with one ROACH2 board. The system described above allowed so far the readout of 16 channels[2] with a white noise level smaller than 35 pA/$\sqrt{\text{Hz}}$, a value compatible with HOLMES requirements.

4 Detector Fabrication

The fabrication of the TES for HOLMES will be accomplished in two separate steps: The first phase, made at NIST (Boulder, CO), involves the deposition of the sensor, the copper structures connected to it, the electrical contacts, and a first 1 µm gold absorber along with a photoresist layer protecting the entire detector except for the absorber area. The detectors are then completed at the INFN section of Genova. Here, the gold absorber is ion-implanted with [163]Ho to reach the target activity. During the implantation, a simultaneous evaporation of gold will run as well. This is intended for two reasons: to control the concentration of [163]Ho and to avoid a saturation effect due to the sputtering of the gold surface due to the impinging [163]Ho nuclei. Simulations made with SRIM (Stopping and Range of Ions in Matter) [10] show that without this co-evaporation, the maximum embeddable amount of [163]Ho

---

[2] The limitation to only 16 channels is due to the usage of just half bandwidth by the firmware currently used.
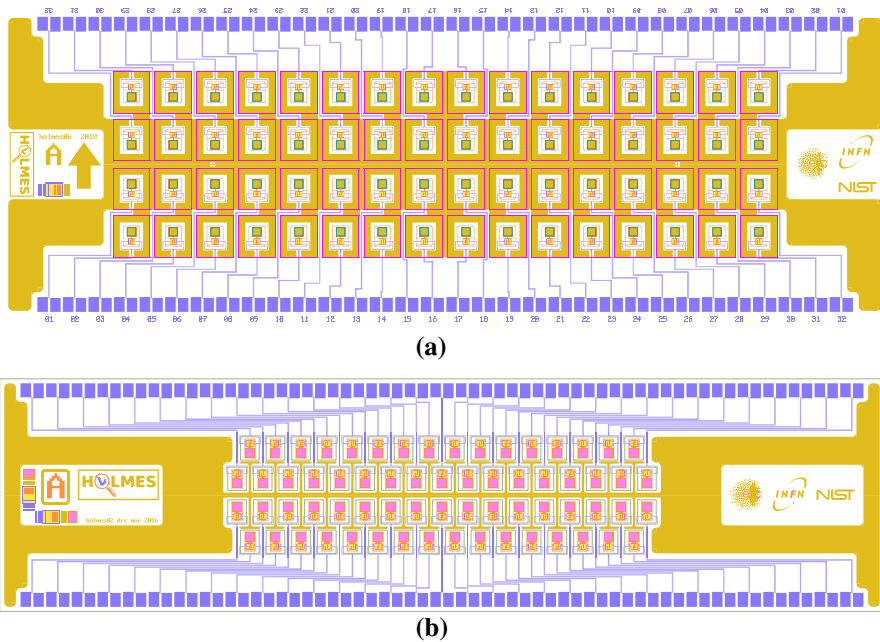
(a)

(b)

Fig. 1 The HOLMES chip featuring 32 TESs each, in the version designed to release the membrane with KOH (**a**) and in the version for the DRIE (**b**): In this latter case, the detectors are placed in a more compact disposition, increasing in this way the geometrical efficiency of the ^{163}Ho implantation (Color figure online)

would be limited to few becquerels. At the end of the implantation, a final 1 µm layer of gold will be deposited *in situ* to avoid oxidation of the ^{163}Ho; the excess gold is then removed by a lift-off procedure. Finally, the membrane is released by etching away the silicon substrate underneath. For this last process, two different processes are being investigated. A wet etching made with KOH has already been set up, while a deep reactive ion etching (DRIE) recipe is still being optimized. This latter technique would allow a chip design with a slightly higher filling factor respect to the KOH (Fig. 1), which is expected to increase the geometrical efficiency of implantation of the ^{163}Ho.

4.1 Source Embedding

The ^{163}Ho nuclei will be embedded in the gold absorbers with a custom ion implanter. It consists of six main components:

- an argon penning sputter-based ion source
- an accelerating section allowing a maximum energy of 50 keV: This energy will allow the ^{163}Ho to implant a few nanometers into the gold
- a magnetic dipole mass analyzer capable of a magnetic field up to 1.1 T. This component is particularly relevant to select only the isotope of interest, avoiding con-
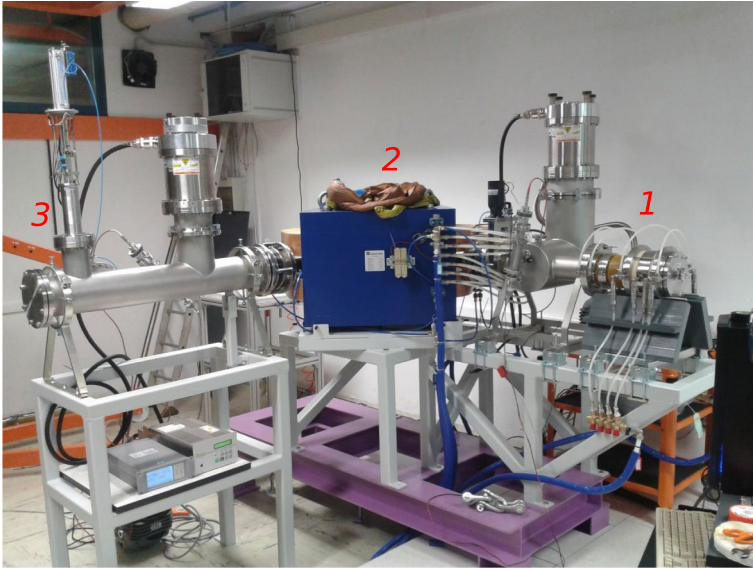
Fig. 2 The custom ion implanter setup at INFN-Genova. From the right to the left: (1) the sputter target and the acceleration section, (2) the magnetic dipole mass analyzer, and (3) the Faraday cup (Color figure online)

taminants such as ^{166m}Ho, a by-product coming from the production of ^{163}Ho which causes an indistinguishable background in the ROI due to its high-energy beta decay. Thanks to this stage, a ^{163}Ho/^{166m}Ho separation better than 5σ is expected

- a focusing stage composed of an electrostatic triplet. This stage will reduce beam diameter to ~ 4 mm FWHM at target position.
- a magnetic scanning stage to deflect the beam in the plane perpendicular to its motion
- the target chamber, where the detectors to be implanted will be hosted. Here, it will also take place the gold evaporation.

While the setup of the target chamber has been optimized in Milano-Bicocca, achieving a gold deposition rate of ~ 50 nm/h with four sputter sources, the setup and optimization of the remaining components of the ion implanter are being carried out at INFN-Genova, where eventually the HOLMES detectors will be ion-implanted and finalized.

The sputter ion source needs a metallic cathode acting as sputter target. The final sputter target will be a sintered compound composed of Ho (5%) in a metallic mixture of Ti (36%), Ni (41%), and Sn (18%) [15]. The first tests have been performed without the focusing stage (Fig. 2) and with a sputter target entirely made of copper. The copper beam current, evaluated with a Faraday cup, reached a value of $\approx 100\,\mu$A. The tests scheduled for the next few months will be

performed with sputter sources made of natural holmium and, eventually, of sintered ^{163}Ho as described above.

5 Background

The presence of background sources can significantly affect the sensitivity of HOLMES. Indeed, any additional background contribution to the spectrum shape can impair the signal due to the neutrino mass. Possible sources are: environmental γ radiation, X-rays, and betas produced in materials close to the detectors, cosmic rays, and radionuclides contaminants (i.e., ^{166m}Ho) in the gold absorber.

A measurement in the HOLMES facility aimed at evaluating the integral intensity of all these contributions, except for the ^{166m}Ho, has been carried out, showing a preliminary background rate in HOLMES-like detectors of $\sim 5 \times 10^{-3}$ counts/sV/day/det in the energy range (1–10) keV. Such intensity has to be compared with the expected magnitude of the unrecognized pileups. The rate of such events would be given by $r_{pp} = A \cdot f_{pp}/2Q$, which, in the case of $A = 300$ Bq/det and $\tau_r = 1\,\mu$s, would give $r_{pp} \approx 1.5$ counts/eV/day/det, significantly higher with respect to the measured background.

6 Pileup Detection Algorithm

The rise time of HOLMES detectors, set by the bandwidth of the bias circuit, is set to be $\sim 14\,\mu$s in order to not exceed the slew rate available. Yet, the effective time resolution can be much shorter than that. Two pileup recognition algorithms are being considered and tested with simulations: Wiener filtering and singular value decomposition (SVD). The pulses were simulated starting from the differential equation governing the TES behavior, and a realistic noise was added. While the Wiener filtering technique has provided a time resolution of 3 μs on pulses with an exponential rise time of 15 μs [16], the latter can possibly improve this result of a further factor 2 [17].

7 Conclusions

HOLMES will measure the neutrino mass with a sensitivity of ~ 2 eV/c^2 collecting 3×10^{13} events from the electron capture of ^{163}Ho. The final detector design has been identified, proving a baseline energy resolution of (4.5 ± 0.3) eV at 2.8 keV with an exponential rise time of 14 μs, a value compatible with a time resolution of few μs. These performances comply with HOLMES requirements in terms of energy and time resolution.

The detector production processes are being set up, while some of them are already optimized. The KOH etching for the membrane release has shown to be applicable to the production of the HOLMES detectors, while an alternative solution based on DRIE is being set up. The target chamber has shown that the gold

deposition rate achievable is compatible with the HOLMES requirements, while the ion implanter is being optimized. To date, a test of the implanter with a target composed of copper has been performed, showing a beam current of $\approx 100\ \mu A$; the subsequent tests, which will be performed in the next few months, will be performed with targets made of natural holmium and, eventually, of ^{163}Ho to produce the proper HOLMES detectors. A first measurement with 16 TESs implanted with ^{163}Ho is expected to start during the year 2020, providing a sensitivity on m_ν of ~ 10 eV/c^2 with a measuring time of 1 month.

References

1. C. Weinheimer, Prog. Part. Nucl. Phys. **48**, 141–150 (2002). https://doi.org/10.1016/S0146-6410(02)00120-5
2. M. Sisti et al., Nucl. Instr. Meth. Phys. Res. A **520**, 125–131 (2004). https://doi.org/10.1016/j.nima.2003.11.273
3. A. Nucciotti, E. Ferri, O. Cremonesi, Astropart. Phys. **34**, 80 (2010). https://doi.org/10.1016/j.astropartphys.2010.05.004
4. E. Ferri et al., J. Low Temp. Phys. **167**, 1035–1040 (2012). https://doi.org/10.1007/s10909-011-0421-6
5. A. de Rújula, M. Lusignoli, Phys. Lett. B **118**, 429 (1982). https://doi.org/10.1016/0370-2693(82)90218-0
6. S. Eliseev et al., Phys. Rev. Lett. **115**, 062501 (2015). https://doi.org/10.1103/PhysRevLett.115.062501
7. B. Alpert et al., Eur. Phys. J. C **75**, 112 (2015). https://doi.org/10.1140/epjc/s10052-015-3329-5
8. A. Puiu et al., J. Low Temp. Phys. (2019). https://doi.org/10.1007/s10909-019-02290-8
9. B. Alpert et al., Eur. Phys. J. C **79**, 304 (2019). https://doi.org/10.1140/epjc/s10052-019-6814-4
10. www.srim.org
11. O. Noroozian et al., Appl. Phys. Lett. **103**, 202602 (2013). https://doi.org/10.1063/1.4829156
12. D.T. Becker et al., J. Instrum. **14**, P10035 (2019). https://doi.org/10.1088/1748-0221/14/10/P10035
13. J. A. B. Mates *PhD. thesis*, Swarthmore College (2004)
14. R. Duan et al., Proc. SPIE **7741**, 77411V (2010). https://doi.org/10.1117/12.856832
15. M. De Gerone et al., Nucl. Instr. Meth. Phys. Res. A **963**, 220–221 (2019). https://doi.org/10.1016/j.nima.2018.10.104
16. E. Ferri et al., J. Low Temp. Phys. **184**, 405 (2016). https://doi.org/10.1007/s10909-015-1466-8
17. B. Alpert et al., J. Low Temp. Phys. **184**, 263 (2016). https://doi.org/10.1007/s10909-015-1402-y

Affiliations

M. Faverzani[1,2] · B. Alpert[3] · M. Balata[4] · D. Backer[3] · D. Bennet[3] ·
A. Bevilaqua[6] · M. Biasotti[5,6] · M. Borghesi[1,2] · G. Ceruti[2] · M. De Gerone[6] ·
R. Dressler[7] · E. Ferri[1,2] · J. Fowler[3] · G. Gallucci[6] · J. Gard[3] · F. Gatti[5,6] ·
A. Giachero[1,2] · S. Heinitz[7,11] · G. Hilton[3] · U. Köster[8] · M. Lusignoli[9] ·
J. Mates[3] · E. Maugeri[7] · S. Nisi[4] · A. Nucciotti[1,2] · L. Parodi[6] · G. Pessina[2] ·
A. Puiu[1,2] · S. Ragazzi[1,2] · C. Reintsema[3] · M. Ribeiro-Gomez[10] · D. Schmidt[3] ·
D. Schumann[7] · F. Siccardi[5,6] · D. Swetz[3] · J. Ullom[3] · L. Vale[3]

[1]   Dipartimento di Fisica, Università di Milano-Bicocca, Milano, Italy

[2]   Istituto Nazionale di Fisica Nucleare, Sezione di Milano-Bicocca, Milano, Italy

[3]   National Institute of Standards and Technology, Boulder, CO, USA

[4]   Laboratori Nazionali del Gran Sasso, INFN, Assergi, AQ, Italy

[5]   Dipartimento di Fisica, Università di Genova, Genova, Italy

[6]   Istituto Nazionale di Fisica Nucleare, Sezione di Genova, Genova, Italy

[7]   Paul Scherrer Institut, Villigen, Switzerland

[8]   Institut Laue-Langevin, Grenoble, France

[9]   Istituto Nazionale di Fisica Nucleare, Sezione di Roma 1, Rome, Italy

[10] Multidisciplinary Centre for Astrophysics (CENTRA-IST), University of Lisbon, Lisbon, Portugal

[11] Present Address: SCK-CEN Mol, Mol, Belgium